

ORIGINAL ARTICLE

Food Engineering, Materials Science, & Nanotechnology

Cytotoxicity, structural, conformational, and techno-functional properties of α -lactalbumin nanostructured aggregates

Jhonatan Rafael de Oliveira Bianchi¹ | Bruna Elisa Reis Paz² |
 Larissa Germano Fonseca² | Rebeca Lima Carvalho² | José Carlos Magalhães¹ |
 Karina Azevedo Pacheco¹ | Andersen Escobar Schlogl² | Daniela Leite Fabrino¹ |
 Edson Romano Nucci¹ | Jane Sélia dos Reis Coimbra³ | Igor José Boggione Santos^{1,2} 

¹Chemical Engineering Graduation Program, Chemistry Engineering Department (DEQUI), Nanotec Research Group – Nanotechnology in Bioprocesses, Universidade Federal de São João del Rei Federal (UFSJ), Alto Paraopeba Campus (CAP), Congonhas, Brazil

²Chemistry, Biotechnology and Bioprocesses Engineering Department, Universidade Federal de São João del Rei (UFSJ), Ouro Branco, Brazil

³Departamento de Tecnologia em Alimentos, Universidad Federal de Viçosa, Viçosa, Brazil

Correspondence

Igor José Boggione Santos, Universidade Federal de São João del Rei (UFSJ), Rod. MG 443, km 7, Ouro Branco, Minas Gerais, Brazil.

Email: igorboggione@ufs.edu.br

Funding information

Centro Nacional de Pesquisa em Energia e Materiais; Fundação de Amparo à Pesquisa do Estado de Minas Gerais; Conselho Nacional de Desenvolvimento Científico e Tecnológico

Abstract

Protein nanostructures can be used in food applications to improve the techno-functional properties of a food formulation. This study aims to find the best conditions for the production and conformational change of α -lactalbumin nanostructured aggregates. The criteria to determine the best operating conditions to produce α -lactalbumin nanostructured aggregates were intensification of foaming and emulsification, techno-functional proprieties, cytotoxic, and antibacterial activity of nanostructures compared with native α -lactalbumin. Conformational alterations occurred in the α -helix and sheet- β protein structures. The size obtained by dynamic light scattering was 163.84 nm with a polydispersity index of 0.29. The nano protein improved the techno-functional property compared to the native protein. Additionally, nanostructures had no cytotoxic effect and were innocuous to bacterial activity. Thus, this study presents the best conditions to produce α -lactalbumin nanostructured aggregates with improved properties that allow new food industry applications.

KEYWORDS

bacterial activity, Box–Behnken methodology, dynamic light scattering, transmission electron microscopy, whey protein

1 | INTRODUCTION

The application of nanotechnology in the food industry has grown over the years due to its potential to bring new physical, chemical, biological, and techno-functional

properties, nutrient absorption, detection, and control of contaminants, controlled release of bioactive compounds, and new sensory properties to food (Liu et al., 2008; Magnuson et al., 2011). In countries such as the United States, Japan, and China, the introduction of nanotechnology

in the dairy industry is already a reality (Chavada, 2016; Shukla, 2012). In this context, nanostructures from milk proteins have gained attention in the food industry (Giroux et al., 2010) due to their high nutritional, functional, and biological value (Fuciños et al., 2021).

Whey protein (WP) is a coproduct of the dairy industry with high nutritional and economic value that comprises a mixture of proteins, mainly globular, highly soluble, and heat-labile (Pereira et al., 2018; Walzem et al., 2002). Bovine α -lactalbumin (α -la) represents 13% of the WP content (Fox et al., 2015); it is a globular protein containing 123 amino acids and a molecular mass of 14.2 kDa (Delavari et al., 2015; Fox et al., 2015), a highly nutritional source of essential and branched amino acids (Kamau et al., 2010), recognized as GRAS (generally recognized as safe) by FDA (Abd El-Salam & El-Shibiny, 2012; Benshitrit et al., 2012), and it has potential antimicrobial, antiviral, anticancer, and immunomodulation activities (León-López et al., 2022).

The interest in using α -la in the food industry is due to its ability to confer diversified techno-functionalities to various products, such as solubility, foaming ability, emulsification, gelification, and film formation. These functionalities influence many food characteristics during processing, storage, preparation, and consumption. They can affect the sensory profile and physical behavior of foods; thus, changes in the techno-functional properties of food ingredients can alter foods and cause economic losses.

Despite the nanometric size of native α -la protein (NAT-ALA), new protein properties can be obtained by restructuring it into nanostructured aggregates, fibrils, nanotubes, and other structures (Hernández et al., 2020; Tarhan & Harsa, 2014). When the protein is nanostructured, the resulting material can be used as an encapsulating agent for bioactive molecules that may degrade during processing, and it can confer new properties to foodstuff. These properties are (i) higher thermal stability in food processing, (ii) increased stability of a food formulation, and (iii) enhanced foodstuff shelf life due to antimicrobial properties (Katouzian & Jafari, 2019).

The nanostructuring of α -la occurs by the reassociation of protein monomers after changes in the external environment following the bottom-up assembly pathway, that is, there is an increase in the hydrodynamic radius (Shimomura & Sawadaishi, 2001). Studies show that obtaining nano protein can occur via enzymatic hydrolysis or altering the ionic strength of the medium. The latter is reached by adding a buffer and salts followed by temperature changes, that is, cold and heat gelation processes (Katouzian & Jafari, 2019). However, the main methods of obtaining α -la nanostructures require expensive reagents,

such as enzymes, so new researchers have been looking for cheaper methodologies to obtain these nanostructures (Fu et al., 2017).

Despite all the innovation potential of nanostructures in the food industry, it is necessary to assess the risk of ingesting nanomaterials present in the food matrix (Galocchio et al., 2015). The α -lactalbumin protein is GRAS and does not have toxicity against normal cell lines like Cho-K1 and NIH/3T3, nor tumoral cells like HeLa and A-549. However, the complex with oleic acid has antitumoral activity (Delgado et al., 2015), due to the oleic acid present. The nanostructure process may change the surface properties, thus investigating the cytotoxicity is necessary for new nanomaterial proteins. Unfortunately, these studies for nano proteins are still incipient in the literature.

Therefore, understanding and finding new methodologies for obtaining simple protein nanostructures and assessing cytotoxicity increases the probability of using these nanostructures in the food industry. Thus, this work aims to develop a method for obtaining and characterizing α -la nanostructured aggregates (NSTs-ALA), their cytotoxicity, antimicrobial activity, and their potential application in the food industry.

2 | MATERIALS AND METHODS

2.1 | Material

The powder of α -lactalbumin (α -la; 95% of protein, which 90% is α -la protein) was kindly donated by Davisco Foods International, Inc. (Eden Prairie, MN, USA). All other chemicals were analytical reagents without any further purification. Distilled water purified via reverse osmosis (Hidrotek, Santa Iria de Azóia, Portugal) was used.

2.2 | Production of α -lactalbumin nanostructured aggregates applying Box-Behnken methodology

A dispersion of α -la nanostructured aggregate (2.00 mg mL^{-1}) was prepared in NaCl aqueous solution. The synthesis of the nanostructure follows 15 experiments of the Box-Behnken design (Table 1) to investigate if the methodology conditions (ionic strength of solvent, time, and temperature) affect the nanostructure hydrodynamic radius and polydispersity index (PDI). The limits of the design variables were adopted in previous works by the Research Group with some modifications (D'Onofre Couto et al., 2021; Hernández et al., 2020). The

TABLE 1 Size chooses by number distribution and polydispersity index (PDI) values obtained through Box–Behnken methodology for nanostructured α -lactalbumin.

Treatment	Temperature (°C)	[NaCl] (mmol L ⁻¹)	Time (min)	Mean size (nm)	Mean PDI
1	25	0	65	329.77 ± 38.59	0.39 ± 0.03
2	50	0	65	679.27 ± 48.88	0.65 ± 0.04
3	25	200	65	179.70 ± 70.74	0.35 ± 0.04
4	50	200	65	501.90 ± 216.85	0.57 ± 0.16
5	25	100	10	163.84 ± 117.25	0.29 ± 0.05
6	50	100	10	30.92 ± 31.10	0.44 ± 0.05
7	25	100	120	511.6 ± 155.45	0.52 ± 0.10
8	50	100	120	430.07 ± 180.23	0.56 ± 0.06
9	37.5	0	10	545.5 ± 303.16	0.61 ± 0.25
10	37.5	200	10	468.87 ± 331.14	0.49 ± 0.21
11	37.5	0	120	275.43 ± 53.90	0.41 ± 0.07
12	37.5	200	120	263.83 ± 64.06	0.37 ± 0.07
13	37.5	100	65	3.41 ± 0.04	0.69 ± 0.28
14	37.5	100	65	3.64 ± 0.12	0.69 ± 0.27
15	37.5	100	65	3.66 ± 0.33	0.58 ± 0.22

independent variables were agitation time (10–120 min), temperature (25–50°C), and NaCl concentration (10–200 mmol L⁻¹). The experiment was conducted in an incubator (Nova Técnica, São Paulo, Brazil). The protein dispersions produced through the method described were stored in a freezer.

After determining the best conditions of temperature, agitation time, and NaCl concentration to obtain the α -la nanostructured aggregates, freezing and thawing cycles of 12 h were carried out to verify the stability of the structure in this process.

2.3 | Nanostructure size distribution

The hydrodynamic radius and PDI were measured by the dynamic light scattering (DLS) technique using a Zetasizer Nano ZS at 25 ± 0.1°C (Malvern, Japan). The samples were measured with no dilution and without any purification in a polystyrene rectangular cell using an avalanche photodiode detector (Brookhaven BI-APD, Holtsville, NY, USA) and a correlator (Turbocort, Brookhaven, GA, USA). The scattered intensity was measured under a detection angle of 173° relative to the source. The light source (CVI Melles Griot, Albuquerque, NM, USA) was a HeNe 35 mW laser with a 632.8 nm wavelength, linearly polarized. A polarized light system was used for intensity control, and the size distribution was determined using the CONTIN algorithm, setting an angle of 173° to measure the dispersion intensity.

2.4 | Characterization of α -la nanostructured aggregates via transmission electron microscopy (TEM) and attenuated total reflectance Fourier transform infrared spectroscopy (ATR-FTIR)

Transmission electron microscopy (TEM) images were obtained with a set of samples by depositing a drop of solution onto 200 mesh copper grids coated with thin films of Formvar carbon (Koch Electron Microscopy, Sao Paulo, Brazil). The samples were dried at 25°C for 24 h, and images were obtained from a transmission electron microscope (Zeiss, 43 model 109, Oberkochen, Germany) at magnitudes of 12,000, 30,000, 50,000, and 85,000× with an accelerating voltage of 80 kV. Size measurements using TEM images were performed using ImageJ software.

Attenuated total reflectance Fourier transform infrared spectroscopy (ATR-FTIR) was performed to investigate the change in the chemical composition of the native protein and α -la nanostructured aggregates. For this purpose, (Agilent, Santa Clara, USA) Cary 360 FTIR equipment was used with the ATR (attenuated total reflection) diamond accessory in the infrared region from 4000 to 650 cm⁻¹.

2.5 | Structural modification of nanostructures

The secondary structures of nanostructures were evaluated by circular dichroism (CD) using a Jasco-810

spectropolarimeter (Jasco Corporation, Tokyo, Japan) equipped with a temperature controller, Peltier-type (PFD 425S, Jasco, Japan) coupled to a thermostatic bath (AWC 100, Julabo, Seelbach, Germany). The spectra were obtained using a quartz cuvette of 1 mm (Hellma Analytics, Müllheim, Germany) at 25°C and a wavelength range of 190–260 nm. Each spectrum was obtained by averaging 10 consecutive readings. Individual solutions of α -la at the same concentrations as nanostructured systems but without heat treatment were used as controls. Deionized water was used as a blank, and the samples were analyzed without dilution. The mean residual ellipticity (MRE) was calculated using the following equation (D'Onofre Couto et al., 2021):

$$MRE = \frac{\theta_{obs}}{10nlC_p} \quad (1)$$

where θ_{obs} is the CD in millidegrees, n is the number of amino acid residues, l is the cell path length in centimeters, and C_p is the mole fraction in dmol cm^{-3} . The deconvolution of the residual molar ellipticity data of the systems was performed using the CONTIN/LL analysis method (Sreerama & Woody, 2000).

The conformational changes of the formed nanostructures were evaluated by fluorescence spectroscopy using a K2 spectrofluorometer (ISS, Baltimore, MD, USA). Samples were analyzed on a 10 mm quartz cuvette (Hellma Analytics, Müllheim im Markgräflerland, Germany) without dilution at 25°C (9001 PolyScience, Warrington, PA, USA). Fluorescence spectra were registered in the 290–450 nm region with an excitation wavelength of 280 nm, which can excite the tryptophan and tyrosine residues (Lakowicz, 2006). Individual solutions of α -la with the same concentrations of the nanostructured systems were used as controls.

2.6 | Techno-functional properties of nanostructures

Proteins can increase their potential in the food industry when nanostructured and used as foam and emulsion stabilizers (Nigen et al., 2009). The techno-functional properties are related to the quality of much-industrialized foods because they influence food's physical-chemical properties. In this sense, the foam and emulsion properties of α -la nanostructures were compared to those of the native protein.

2.6.1 | Foaming ability

The foaming ability of conjugates was evaluated by measuring the total volume and foam volume immediately after homogenization, according to Equation (2) (D'Onofre Couto et al., 2021). Samples (5 mL) were homogenized in IKA Ultra Turrax (T25 digital, IKA, Königswinter, Germany) for 1 min at 13,500 rpm:

$$VI = \frac{V_T - V_T}{V_F} \times 100 \quad (2)$$

where VI (%) is the volume increase, V_T is the protein suspension volume before agitation (mL), and V_F is the protein suspension volume after agitation (mL).

The foam stability (FS) of the nanostructures was measured immediately after stirring and at 5 min intervals until 30, 60, and 120 min at 25°C. The FS percentage was obtained by the following equation (D'Onofre Couto et al., 2021):

$$FS = \frac{V_{FT}}{V_{F0}} \times 100 \quad (3)$$

where V_{FT} is the foam volume after time t , and V_{F0} is the foam volume at time 0.

2.6.2 | Emulsifying properties

The method proposed by Shi et al. (2021) was used with modifications (Shi et al., 2021). The oil-in-water emulsion was prepared in a three-to-one proportion of sunflower oil and nanostructures of α -lactalbumin dispersions under the best conditions obtained through the Box-Behnken methodology described in Section 2.1. The emulsions were homogenized at 14,000 rpm in an Ultra Turrax (Biovera, Sao Paulo, Brazil) homogenizer for 1 min at 25°C. Then, emulsion aliquots were diluted in sodium dodecyl sulfate 0.1% (w/v) at different times (0, 5, 15, and 30 min). After this, the diluted emulsion absorptions were measured at 500 nm in a UV-Vis spectrophotometer (Shimadzu, Kyoto, Japan). The emulsifying activity index (EAI) and emulsion stability index (ESI) were obtained through the following equations (Shi et al., 2021):

$$EAI (\text{m}^2\text{g}^{-1}) = \frac{2 \times 2.303 \times A_0 \times D_F}{c \times (1 - \theta) \times 1000} \quad (4)$$

$$ESI (\text{min}) = \frac{A_0}{A_0 - A_{30}} \times 30 \quad (5)$$

A_0 is the diluted emulsion absorption at time 0, A_{30} is the absorption at 30 min, D_F is the dilution factor, c is the initial protein concentration (mg mL^{-1}), and θ is the oil fraction required to form an emulsion (0.25).

2.7 | Cytotoxic and antibacterial activity of nanostructures

2.7.1 | Cytotoxicity assay in mammalian cells

Vero mammalian cells were used for cytotoxicity analysis. These mammalian cells had continuous lineage fibroblasts derived from a green monkey kidney (*Cercopithecus aethiops*). Cultures were maintained in Dulbecco's modified minimal essential medium with 5% fetal bovine serum (FBS) and an antibiotic cocktail composed of gentamicin (50 g mL^{-1}), penicillin potassium (200 U mL^{-1}), and fungizone (2.5 g mL^{-1}). Cells were maintained at 37°C in a CO_2 oven and were harvested with a 3.5-day interval using trypsin solution EDTA ($136 \text{ mmol L}^{-1} \text{ NaCl}$; $5 \text{ mmol L}^{-1} \text{ KCl}$; $55 \text{ mmol L}^{-1} \text{ glucose}$; $69 \text{ mmol L}^{-1} \text{ NaHCO}_3$; 0.5 g v^{-1} trypsin 1: 250 (Difco); $0.5 \text{ mmol L}^{-1} \text{ EDTA}$; 1% phenol red) (da S. Fernandes, 2021).

For the cytotoxicity assay, nanostructures were submitted to the cytotoxicity test. The nanostructure dispersion used in the assay was 2.0 and 1.0 mg mL^{-1} α -la. The added volumes of the dispersions in the microplate lines were 1, 0.5, 0.25, 0.125, 0.062, 0.031, 0.016, and 0.007 mL , which generated concentrations of nanostructures of 0.02, 0.01, 0.005, 0.0025, 0.00124, 0.00062, 0.00032, and $0.00014 \text{ mg mL}^{-1}$ for dispersion stock 2.0 mg mL^{-1} α -la, and 0.01, 0.005, 0.0025, 0.00125, 0.00062, 0.00031, 0.00016, and $0.00007 \text{ mg mL}^{-1}$ for dispersion stock 1.0 mg mL^{-1} α -la. Cells were distributed into 96 well microplates (4×10^5 cells ($100 \mu\text{L well}^{-1}$)) and incubated at 37°C for 24 h. Then, $100 \mu\text{L well}^{-1}$ complete medium with 2% FBS and different compound concentrations were added in triplicate. The plates were incubated for 48 h, and then $25 \mu\text{L}$ of 3-(4,5-dimethylthiazol-2-yl)-2,5-diphenyltetrazol bromide solution (2 mg mL^{-1} in PBS) was added at 37°C for 90 min. A volume of $130 \mu\text{L}$ dimethyl sulfoxide (DMSO) per well was added to dissolve the formazan crystals by keeping the cultures under 150 rpm stirring for 15 min. The good absorbances were determined using an ELISA spectrophotometer ($\lambda = 492 \text{ nm}$).

It should be said in the highlight that none of the concentrations tested was toxic and; therefore, CC50 could not be determined. Although the technique was used to investigate the cytotoxic concentration for 50% of the treated

cells, cytotoxicity was not detected, as it was 0%, even at the highest concentration used. Cell toxicity was expressed in CC50 terms. The viable cell percentage was calculated as $[(B \cdot 100)/A]$, where A and B are the absorbances at 492 nm of the wells with untreated (A) cells and treated (B) cells, respectively.

2.7.2 | Microorganisms used in the antimicrobial action tests

The microorganisms used were gram-positive *Staphylococcus aureus* (ATCC 29,213), *Bacillus cereus* (ATCC 11,778), gram-negative *Klebsiella pneumoniae* (ATCC 4352), and *Salmonella typhimurium* (ATCC 14,028).

2.7.3 | Minimum inhibitory concentration (MIC)

To determine the compound's lowest concentration that would inhibit bacterial growth, the broth dilution method, recommended by the National Health Surveillance Agency, was used, following the Manual Clinical and Laboratory Standards Institute (CLSI) protocols with adaptations (CLSI, 2015).

The inoculum was adjusted to 0.5 on the MacFarland scale and diluted 100-fold from the mixture of colonies grown for 24 h in nutrient broth. A $50 \mu\text{L}$ final inoculum volume plus the nutrient broth solution ($50 \mu\text{L}$) was placed in each well of a 96-well plate, and the test substance was twice the desired concentration. All tests were performed in triplicate using different controls, such as the medium control, inoculum control, negative control (vehicle), and streptomycin antibiotics positive control, at concentrations from 5000 to $10.5 \mu\text{g mL}^{-1}$, with a dilution factor in each well of two times. Turbidity was observed after a 24 h incubation time to detect bacterial growth.

2.8 | Statistical analysis

The results obtained were analyzed using Excel 2016 software with a confidence level of 95%. The nanostructure size data resulting from the DLS method were organized through the Box-Behnken technique to find the best production conditions for the nanostructures. The F statistical test and Pareto graph analysis gave the best experimental conditions. After these analyses, the response surfaces were generated. Pareto charts and response surfaces were generated using SPSS Statistics software (Version 7.0, SPSS Inc. Chicago, IL, USA). A Tukey test with a 5% significance level was performed with 2016 Excel software.

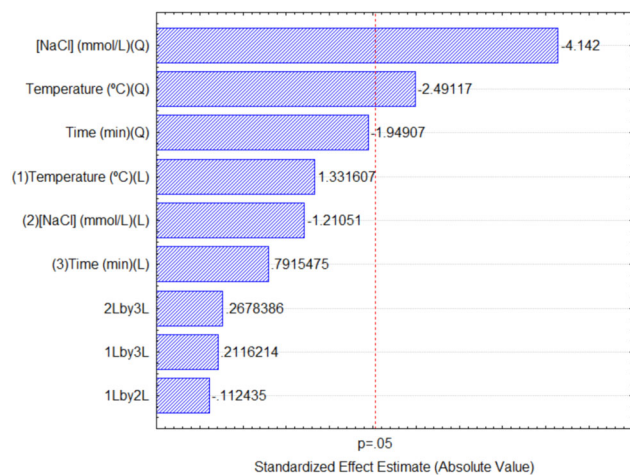


FIGURE 1 Pareto's chart of standardized effects with size (nm) as a dependent variable, 3 level factors, 45 runs, and 1 block.

3 | RESULTS AND DISCUSSION

3.1 | Production of α -la nanostructured aggregates applying the Box–Behnken methodology

Milk WPs can form new structures with differentiated functionalities, such as nanometric structures, through their conformation, surface, size, and net charge characteristics. Thus, different medium physical–chemical conditions, such as temperature, pH, heating time, and ionic force, change the attractive and repulsive forces, resulting in self-association among hydrolyzed proteins for transformation into structurally distinct aggregates (Kimpel & Schmitt, 2015).

Table 1 shows the size distribution (number distribution) and PDI values as response variables of the Box–Behnken methodology. The size distribution was kept in nanometers for all treatments, implying a size modification caused by the independent variables. Additionally, the PDI showed a good protein population distribution in the solution. The Box–Behnken methodology was used to indicate the best combination of variables (temperature, NaCl concentration, and agitation time) to form the nanostructures.

Figure 1 shows the Pareto chart ($p < 0.05$); the analysis of the effects showed that the NaCl concentration and the temperature are significant for nanostructure production. As in this work range, some factors are significant in the final response of the analysis; it is possible to build a model to predict the result. The ANOVA analysis shows that the model is significant for predicting the result, that is, with this equation it is possible to optimize the nanostructure synthesis process by determining the best conditions for temperature and NaCl concentration (supplemental file,

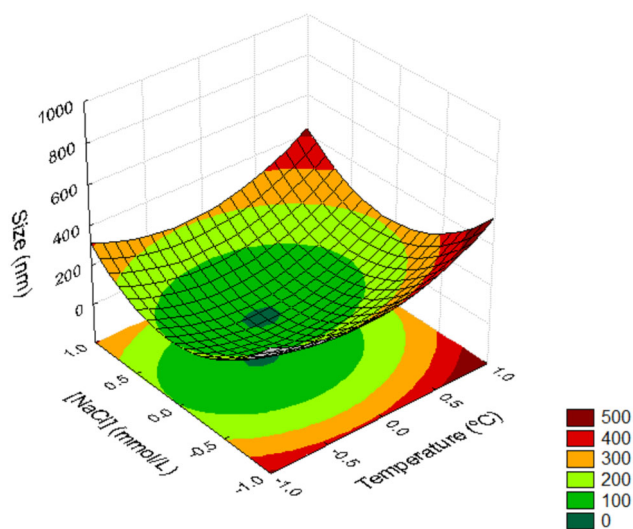


FIGURE 2 Response Surface shows the relationship between the dependent variable, size, and the independent variable for the Box–Behnken methodology; NaCl concentration and temperature variables.

Tables S1 and S2). However, in this work, the process optimization was not carried out, instead it was used the surface methodology.

The literature points out that a nanostructure size ranging from 1 to 300 nm (Arroyo-Maya et al., 2012) and a PDI index smaller than 0.4 are desired (Madalena et al., 2016). The NaCl in the α -la solution creates a stressful environment that allows protein denaturation and posterior aggregation in nanostructures. The formation of nanostructures occurs when it is the most stable conformation (Yu et al., 2022). To understand the influence of temperature and NaCl concentration, the surface methodology was used. As shown in Figure 2, the production conditions affect the nanostructure size. The crossing green region is the best once they produce nanostructure sizes between 100 and 200 nm. Therefore, the 100 mmol L⁻¹ concentration of NaCl was chosen as the best ionic force condition to produce the protein nanostructures.

Furthermore, heat causes conformational deformation in protein secondary and tertiary structures (Relkin & Mulvihill, 1996); however, the ambient temperature (25°C) was chosen as the best condition once the surface region is also favorable to nanostructure processes and also to save energy and avoid process safety concerns related to high temperatures.

Once the agitation time was not a significant parameter, nanostructure production of 10 min was used; therefore, the best production conditions were 10 min of agitation time, ambient temperature (25°C), and 100 mmol L⁻¹ NaCl concentration. Thereby as proof of concept, the synthesis was carried out in the established best conditions and led

to nanostructure sizes of 163.84 nm and PDI values of 0.29, which are in the appropriate range for both parameters. It is worth noting that the process used in the present work is simple and inexpensive. For instance, 2014 synthesized α -la nanotubes with 20–100 nm sizes by solubilizing native protein in Tris-HCl 75 mmol L⁻¹ buffer at pH 7.5 in the presence of CaCl₂ in proportions of 2:1 and 4% (w/w) BLP. The systems were then incubated at 50°C (Tarhan & Harsa, 2014).

The freezing of the protein immediately after obtaining the nanostructure was performed because the pretest results pointed out the reduction of large aggregates under freezing. The sizes of the samples stored at 25°C and after 1, 2, and 3 freeze-thaw cycles were 193.90 ± 66.04, 3.71 ± 0.46, and 4.23 ± 0.94 nm with PDI values of 0.31 ± 0.06, 0.98 ± 0.03, and 0.82 ± 0.01, respectively. In general, the freeze-thaw destabilization of nano protein size can occur by the crystallization of the water phase and by changes in the chemical environment of the protein, such as ionic strength and changes in pH (Degner et al., 2014). Thus, it is suggested that the formation of aggregated nanostructures occurred in the first freeze-thaw cycle. Most likely, changes in the chemical environment promoted by the presence of NaCl and during the growth of ice crystals from the water favor the size decrease of dispersions at 25°C (Feng et al., 2020; Yu et al., 2022). From the second freeze/thaw cycle, the aggregates found a chemical environment more favorable to the approximate size of the native protein. Therefore, it is necessary to study future mechanisms of stabilization of the aggregated nanostructures obtained after the second freeze/thaw cycle with the addition of stabilizer molecules.

3.2 | Characterization of α -la nanostructured aggregates via transmission electron microscopy (TEM) and attenuated total reflectance Fourier transform infrared spectroscopy (ATR-FTIR)

Figure 3 shows the TEM of the synthesized α -lactalbumin nanostructures. The mean size was 10.16 ± 3.38 nm, as calculated by ImageJ. The difference between the sizes obtained by DLS and TEM can be justified because DLS measures the hydrodynamic radius, and TEM measures the dry structure (Souza et al., 2016). In DLS, because of the aggregation of proteins in an aqueous solution, the protein molecules seek lower thermodynamic energy, which can happen with the interactions among the sulfidic groups (Kolakowski et al., 2001; Madalena et al., 2016). When drying the colloidal dispersion for use in TEM, it is possible that the protein has undergone changes in confor-

mation and sought a more favorable state with molecular interactions of hydrophilic portions that were previously interacting with the solvent, so it was compacted, exposing the hydrophobic regions, suggesting a crystallization process, which is reaffirmed by the TEM images (Figure 3) showing a nonglobular structure, more commonly viewed when this molecule is not pure, as reviewed by Cuevas-Gómez et al. (2021) and shown by Nigen et al. (2009), who combined α -la with lysozyme and obtained spherical nano proteins, observing the influence of the medium's electrostatic force on the behavior of the bottom-up nanostructuring, and Arroyo-Maya et al. (2012) using ketone as solvent.

The FTIR spectral changes were assessed by principal component analysis in the amide I and II regions (1750–1350 cm⁻¹). Figure 4 shows the FTIR spectra of native α -la and α -la nanostructured aggregates, and the major bands detected were analyzed by using data from Kher et al. (2007), Tarhan et al. (2021), and Zhang et al. (2014). The broad regions observed for native α -la were the amide I band at 1637 cm⁻¹, COO⁻ antisymmetric stretching bands at approximately 1542–1509 cm⁻¹ overlapping with the amide II band at ~1550 cm⁻¹, CH₂ bending vibration band at ~1458 cm⁻¹, and COO⁻ symmetric stretching band at approximately 1390 cm⁻¹. These broad regions are sensitive to the protein secondary structure (Zhong et al., 1999). The α -helix, β -sheet, and random structures existing in native α -la protein were detected at 1632–1649, 1527–1542, and 1640–1650 cm⁻¹, respectively.

The infrared spectrum of the α -la nanostructured aggregates has the same main bands reported above; however, with a lower intensity, a higher bandwidth with shoulders at higher frequencies, and a small shift from the maximum absorption band to higher wave numbers. This behavior may suggest a greater exposure of the α -helix structure to the solvent and protein denaturation (Zhong et al., 1999).

The percentage of secondary structure was calculated by the curve under each corresponding peak using the second derivative method (Yang et al., 2015). In the native α -la, the results showed 38.53% of α -helix, 4.76% of β -sheet, and 21.10% of the random structure. The nanostructured α -la has a reduced α -helix and β -sheet structure (28.35% and 1.96%, respectively). The random increase to 23.33%. However, the CD was used to confirm the results as described in the following section.

3.3 | Circular dichroism and fluorescence analysis

CD data were used to assess modifications in the secondary structure of the protein. Figure 5 shows native α -la, α -la with NaCl, and nanostructured protein CD

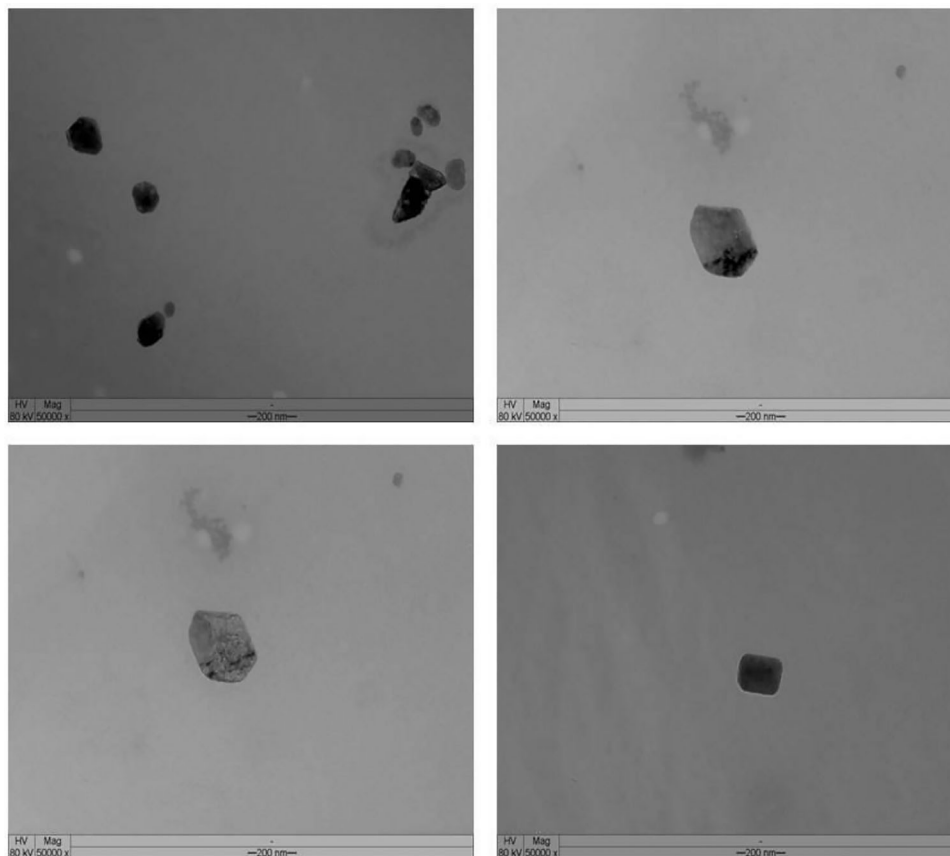


FIGURE 3 Representative images of electron microscopy from the synthesized α -lactalbumin nanoparticles demonstrating a crystal-like morphology. The nanostructures exhibit sharpened surfaces that can be occurred due to the changes in conformation and sought a more favorable state. Scale bar = 200 nm.

spectra. The native α -la spectrum presents a negative peak between 205 and 225 nm and one positive bound at 190 nm, indicating α -helical protein, typical results of α -la, with two minimum bands at approximately 208 and 222 nm (Hernández et al., 2020). In addition, a negative broadband at 218 nm and a positive band at 195 nm indicate a β -sheet structure (Tarhan et al., 2021). Thus, the treatments performed with the protein did not change the spectrum shape or its displacement. This fact was proven in the data deconvolution.

The deconvolution of CD data using the CONTIN analysis method showed that the secondary structure for α -la nanostructured is formed by α -helix 36.8%, β -sheet 8.3%, turns 22.3%, and disordered structure 32.5%. All treatments increased the α -helix structure percentage to 37.7% and reduced the β -sheet to 7.7%. Additionally, the turn structure was around 21.9% for α -la with NaCl. Moreover, the disorder for α -la with NaCl and α -la nanostructured aggregate was 32.7%.

Therefore, the agitation and ionic strength cause few changes in the protein's secondary structure. A similar result was obtained by Graveland-Bikker et al. (2009) who obtained α -la nanotubes via enzymes and Hu et al. (2019)

who obtained α -lactalbumin-based micellar nanoassemblies, respectively, whose CD spectrum showed significant conformational changes but maintained the secondary structure (Graveland-Bikker et al., 2009; Hu et al., 2019). Monteiro et al. (2016) also reported similar results for α -la-Lys supramolecular structures prepared at pH 11 and 25°C for 15 and 35 min (Monteiro et al., 2016). Thus, the ionic strength alteration probably forced the protein recombination that aggregates and forms nanostructures in a bottom-up pathway (Ipsen & Otte, 2007).

Figure 6 shows the fluorescence intensity of protein structures, which allows the protein tertiary structure to be evaluated. The native protein showed a peak at approximately 320 nm, indicating exposed tryptophan (Trp) and tyrosine (Tyr). Similar results were obtained by Hernández, et al. (2020) for the native protein. The native form is a naturally fluorescent protein because of four tryptophan residues at positions 26, 60, 104, and 118 nm (Katouzian et al., 2020).

The α -la with NaCl showed similar behavior, resulting in a peak of FI higher than the native protein. This result suggested that with the increase in ionic strength, ions remove water molecules from the solvation layer,

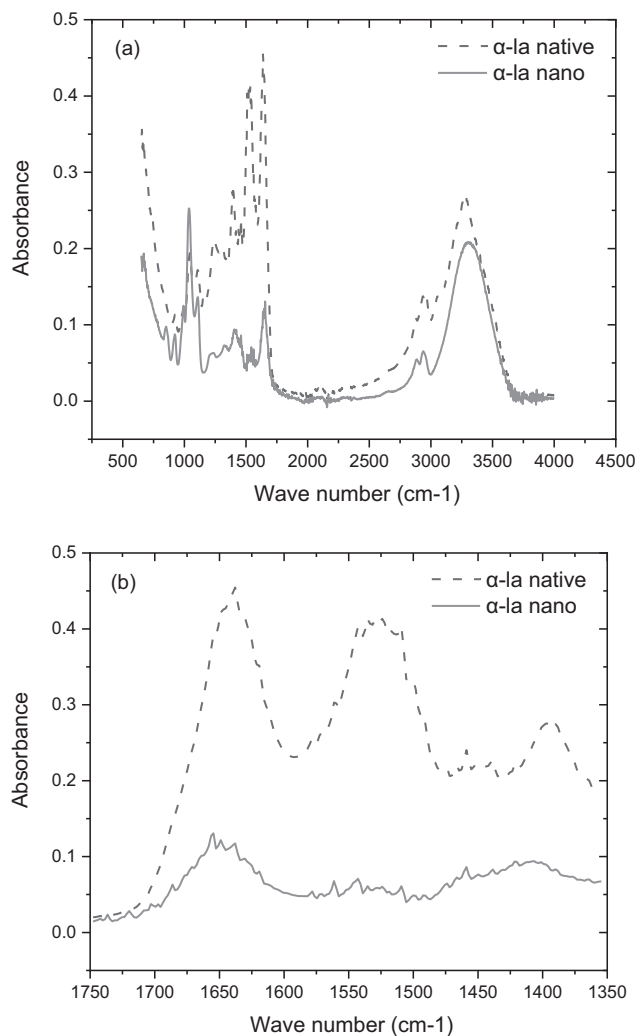


FIGURE 4 The Fourier transform infrared spectroscopy (FTIR) spectra of native α -la and α -la nanostructured aggregates in the infrared region from (A) 4000 to 650 cm^{-1} and (B) 1750 to 1350 cm^{-1} .

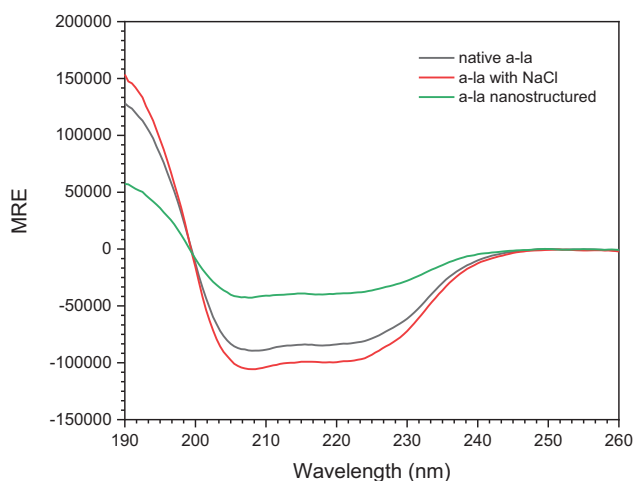


FIGURE 5 Circular dichroism of α -lactalbumin structures as a function of the wavelength.

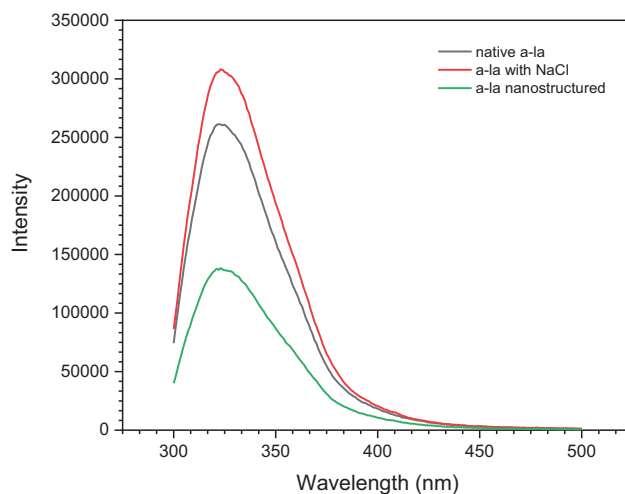


FIGURE 6 Fluorescence of α -lactalbumin structures as a function of the wavelength.

causing proteins to aggregate through the hydrophobic regions and exposing the hydrophilic regions to the medium. Furthermore, the exposure of hydrophilic regions exposes chromophores, increasing the intensity of fluorescence (Liu et al., 2016; Monteiro et al., 2016).

On the other hand, α -la nanostructure showed a peak with less intensity. This behavior suggests that the protein conformation change caused the chromophores' amino acids to go to hydrophobic regions, not exposed to the more polar environment (Monteiro et al., 2016); these results shed light on the characterization presented in this work (Figure 6). This same behavior was observed by Diniz et al. (2014), in which the α -la native structure showed a higher peak of the fluorescence spectrum compared to glycomacropptide (Diniz et al., 2014). The results obtained agree with the change in the secondary structure observed using the CD technique. Therefore, the nanostructure formation process contributes to the randomization of the protein tertiary structure. The randomization of the protein tertiary structure indicates protein denaturation. Consequently, the nanostructures were indeed formed.

3.4 | Techno-functional properties

3.4.1 | Foaming properties

The foam formed in a protein solution occurs due to volume expansion resulting from the air addition in the medium by the agitation of the protein dispersion. Foam formation is related to many factors, such as solubility, salt presence, nature, and protein denaturation state. The FS measures the protein's ability to stabilize the

TABLE 2 Volume increase (VI) and foam stability (FS) data at 30, 60, and 120 min.

	Nanostructure	Protein + NaCl
VI (%)	45.00 ^a ± 8.66	38.33 ^a ± 7.64
FS0 (%)	45.00 ^a ± 8.66	38.33 ^a ± 7.64
FS30 (%)	14.76 ^a ± 5.02	19.44 ^a ± 3.92
FS60 (%)	0.00 ^a ± 0.00	11.80 ^b ± 0.98
FS120 (%)	0.00 ± 0.00	0.00 ± 0.00

Note: Values with the same letter were not significantly different by Tukey's test ($p < 0.05$). The measurements were performed in triplicate. The Tukey test shows the significance between values obtained from different sample conditions at the same resting time.

interface around the air bubbles, retaining the maximum foam volume (Santos et al., 2019).

Table 2 shows the foam property results calculated for the systems containing native α -la, nanostructured α -la, and native α -la in the presence of NaCl (α -la + NaCl). The Tukey test showed a significant difference in the FS, at 60 min, for nanostructure α -la and native α -la + NaCl. There was no significant difference between the three variations analyzed at other times. The FS values at time t (FS t) of nanostructured α -la and α -la in NaCl presence had similarities, slowly reducing with time. However, from 60 to 120 min, there was no foam in the medium. Therefore, the nanostructures did not significantly increase the FS compared to the NaCl protein dispersion.

3.4.2 | Emulsifying properties

The emulsion absorption was applied in Equations (3) and (4) to obtain the EAI and ESI parameters. The results are presented in Table 3.

After performing the Tukey test, it was verified that the parameters evaluated for the emulsion techno-functional property showed a significant difference for the sample with nanostructured protein compared with the protein in a NaCl solution. The nanostructures showed higher emulsifying activity and better emulsion stability at 15 and 30 min times than the protein solution in NaCl.

Rodiles-López et al. (2008) studied α -lactalbumin emulsifying properties and obtained a stability of 11.7 for 5 min and a 106 EAI value for the native protein at a 40°C thermal treatment (Rodiles-López et al., 2008). The EAI value found in this study was smaller than that found by Rodiles-López et al. (2008), but the ESI parameter is more critical for the food industry; it indicates the structural capacity to stabilize emulsions, resulting in a uniform

appearance product. A higher ESI value is better because it indicates a stability increase because of the hydrophobicity and efficiency of reducing the interface's surface tension (Lajnaf et al., 2020). Based on Table 3, as time increases, the stability of a sample containing nanostructures also increases. Therefore, time was significant to the nanostructure's diffusion to the oil–water interface, contributing to the nanostructure's surfactant action. For the protein system in the presence of NaCl, the best stability obtained was at 30 min.

3.5 | Cytotoxic and antibacterial activity of nanostructures

Minimum inhibitory concentration (MIC) assays were performed to assess the toxicity of the α -lactalbumin nanoparticles. The MIC is the lowest concentration capable of completely inhibiting bacterial growth.

There was no change in microorganism growth. The control wells' expected bacterial growth was excellent, and the medium was carefully controlled, confirming that there was no contamination, thus designing an excellent comparison between the experimental and control wells. The positive control was performed with streptomycin antibiotic, in which the MIC was impossible to obtain because all concentrations of the antibiotic inhibited growth (from 5000 to 10.5 $\mu\text{g mL}^{-1}$).

Medium turbidity was observed in the wells with bacterial presence (Figure S1), indicating bacterial growth. Therefore, there was no antibacterial activity for the milk-derived nanoparticles, at least for the bacteria tested, *S. aureus*, *B. cereus*, *K. pneumoniae*, and *S. typhimurium*.

3.6 | Cytotoxic activity evaluation of nanostructures

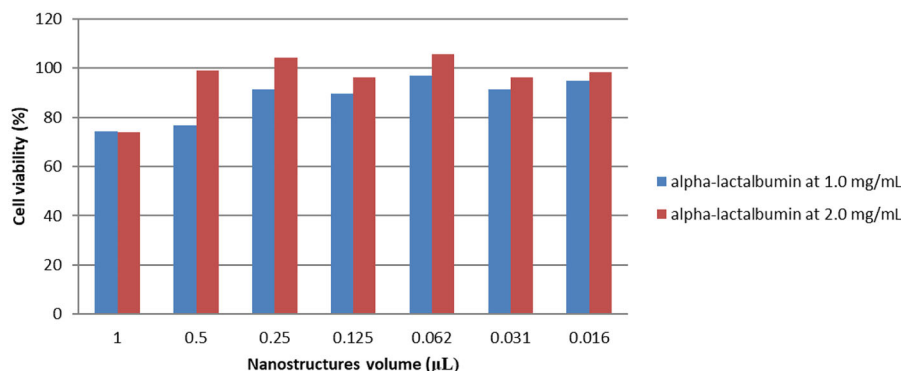
MTT (2-[4,5-dimethylthiazol-2-yl]-2,5 diphenyl tetrazolium bromide) assays were performed to evaluate α -lactalbumin nanoparticle cytotoxicity in Vero mammalian cells. Data analysis was weighted as 100% of the mean live cells in the microwells that did not contain the nanostructures. The compound concentration capable of reducing the optical density of treated cells by 50% compared to the control was determined by calculating the cytotoxic concentration of 50% of the cells (CC50), and the result is expressed in Figure 7.

In the obtained results, we can observe that lower CC50 values were obtained when the nanostructure volume was 1.0 μL (0.02 mg mL^{-1} for α -lactalbumin stock of 2.0 and 0.01 mg mL^{-1} for α -lactalbumin stock of 1.0 mg mL^{-1}), although none of them was less than 50%.

TABLE 3 Emulsion stability index (ESI) and emulsifying activity index (EAI) results for the two emulsions prepared.

Sample	EAI ($\text{m}^2 \text{g}^{-1}$)	ESI5 (min)	ESI15 (min)	ESI30 (min)
Nanostructures	$2.106^a \pm 0.078$	$7.135^a \pm 0.134$	$48.420^a \pm 12.687$	$40.825^a \pm 4.965$
Protein + NaCl	$0.457^b \pm 0.039$	$10.982^b \pm 1.389$	$25.072^b \pm 0.986$	$27.320^b \pm 1.720$

Note: Values with the same letter were not significantly different by Tukey's test ($p < 0.05$). The measurements were performed in triplicate.

**FIGURE 7** Vero cells viability after 48 h in the milk serum-derived nanoparticles presence, as determined by the MTT metabolism assay.

Based on these results, we can conclude that nanoparticles derived from WP are not toxic to Vero cells at any concentration.

4 | CONCLUSION

The methodology proposed indicates the feasibility of forming α -lactalbumin nanostructures by changing the medium's ionic strength and mechanical agitation. This process resulted in nano α -la with an almost spherical shape. Conformational alterations in the structures of the α -helix and β -helix of α -la nanostructures were verified through dichroism and fluorescence techniques. The thermal properties were maintained. The nanostructured proteins formed emulsions with higher emulsifying activity and better emulsion stability than emulsions from NaCl protein solution. The cytotoxicity study at the concentrations evaluated showed that α -lactalbumin nanostructures did not present any cytotoxic effect on mammalian Vero cells. The antibacterial assay considering the *S. aureus*, *B. cereus*, *K. pneumoniae*, and *S. typhimurium* bacteria showed that nanoparticles also have innocuous antibacterial activity. Therefore, α -la nanostructures have the potential to be applied to the formulation of food with nutraceutical properties.

AUTHOR CONTRIBUTIONS

Jhonatan Rafael de Oliveira Bianchi: Investigation; writing—review & editing; data curation. **Bruna Elisa**

Reis Paz: Investigation. **Larissa Germano Fonseca:** Investigation. **Rebeca Lima de Carvalho:** Investigation. **José Carlos Magalhães:** Investigation; data curation. **Karina Azevedo Pacheco:** Investigation. **Andersen Escobar Schlogl:** Investigation. **Daniela Leite Fabrino:** Writing—review & editing; data curation. **Edson Romano Nucci:** Writing—review & editing; data curation. **Jane Sélia dos Reis Coimbra:** Resoucers; conceptualization. **Igor José Boggione Santos:** Conceptualization; methodology; supervision; investigation; writing—review & editing.

ACKNOWLEDGMENTS

The authors thank the Conselho Nacional de Pesquisa e Desenvolvimento Tecnológico (CNPq), the Coordenação de Aperfeiçoamento de Pessoal de Nível Superior—Brazil (CAPES), and the Fundação de Amparo à Pesquisa do Estado de Minas Gerais (FAPEMIG) for the financial support, and Núcleo de Microscopia e Microanálise of Universidade Federal de Viçosa, the Brazilian Biosciences National Laboratory—Spectroscopy and Calorimetry Laboratory (LNBio) of the National Center for Research in Energy and Materials (CNPEM), CIPHARMA (Programa de Pós-Graduação em Ciências Farmacêuticas, UFOP), and Davisco Food International for their support for this work.

CONFLICT OF INTEREST STATEMENT

The authors declare no competing financial interest.

ORCID

Igor José Boggione Santos  <https://orcid.org/0000-0001-6583-3589>

REFERENCES

- Abd El-Salam, M. H., & El-Shibiny, S. (2012). Formation and potential uses of milk proteins as nano delivery vehicles for nutraceuticals: A review. *International Journal of Dairy Technology*, 65(1), 13–21. <https://doi.org/10.1111/j.1471-0307.2011.00737.x>
- Arroyo-Maya, I. J., Rodiles-López, J. O., Cornejo-Mazón, M., Gutiérrez-López, G. F., Hernández-Arana, A., Toledo-Núñez, C., Barbosa-Cánovas, G. V., Flores-Flores, J. O., & Hernández-Sánchez, H. (2012). Effect of different treatments on the ability of α -lactalbumin to form nanoparticles. *Journal of Dairy Science*, 95(11), 6204–6214. <https://doi.org/10.3168/jds.2011-5103>
- Benshitrit, R. C., Levi, C. S., Tal, S. L., Shimoni, E., & Lesmes, U. (2012). Development of oral food-grade delivery systems: Current knowledge and future challenges. *Food & Function*, 3(1), 10–21. <https://doi.org/10.1039/C1FO10068H>
- Chavada, P. J. (2016). Novel application of nanotechnology in dairy and food industry: Nano inside. *International Journal of Agriculture Sciences*, 8, 2920–2922.
- Cuevas-Gómez, A. P., Arroyo-Maya, I. J., & Humberto, H.-S. (2021). Use of α -lactalbumin [α -La] from whey as a vehicle for bioactive compounds in food technology and pharmaceuticals: A review. *Recent Progress in Materials*, 3(2), 1.
- Fernandes, D. G. da S., Andrade, V. B., Lucena, L. N., Ambrosio, F. N., de Souza, A. L. M., Batista, B. L., Rolim, W. R., Seabra, A. B., Lombello, C. B., da Silva, F. D., & Garcia, W. (2021). Cytotoxicity and antimicrobial properties of photosynthesized silver chloride nanoparticles using plant extract from stryphnodendron adstringens (Martius) coville. *Journal of Cluster Science*, 33(2), 687–695. <https://doi.org/10.1007/s10876-021-02011-w>
- Degner, B. M., Chung, C., Schlegel, V., Hutkins, R., & McClements, D. J. (2014). Factors influencing the freeze-thaw stability of emulsion-based foods. *Comprehensive Reviews in Food Science and Food Safety*, 13(2), 98–113. <https://doi.org/10.1111/1541-4337.12050>
- Delavari, B., Saboury, A. A., Atri, M. S., Ghasemi, A., Bigdeli, B., Khammari, A., Maghami, P., Moosavi-Movahedi, A. A., Haertlé, T., & Goliaei, B. (2015). Alpha-lactalbumin: A new carrier for vitamin D3 food enrichment. *Food Hydrocolloids*, 45, 124–131. <https://doi.org/10.1016/j.foodhyd.2014.10.017>
- Diniz, R. S., dos Reis Coimbra, J. S., Teixeira, Á. V. N. D. C., da Costa, A. R., Santos, I. J. B., Bressan, G. C., da Cruz Rodrigues, A. M., & da Silva, L. H. M. (2014). Production, characterization and foamability of α -lactalbumin/glycomacropptide supramolecular structures. *Food Research International*, 64, 157–165. <https://doi.org/10.1016/j.foodres.2014.05.079>
- D'Onofre Couto, B., Novaes da Costa, R., Castro Laurindo, W., Moraes da Silva, H., Rocha da Silva, C., Sélia dos Reis Coimbra, J., Barbosa Mageste, A., de Cássia Dias, S., & José Boggione Santos, I. (2021). Characterization, techno-functional properties, and encapsulation efficiency of self-assembled β -lactoglobulin nanostructures. *Food Chemistry*, 356, 129719. <https://doi.org/10.1016/j.foodchem.2021.129719>
- Feng, H., Jin, H., Gao, Y., Yan, S., Zhang, Y., Zhao, Q., & Xu, J. (2020). Effects of freeze-thaw cycles on the structure and emulsifying properties of peanut protein isolates. *Food Chemistry*, 330, 127215. <https://doi.org/10.1016/j.foodchem.2020.127215>
- Fox, P. F., Uniacke-Lowe, T., McSweeney, P. L. H., & O'Mahony, J. A. (2015). Milk proteins. In *Dairy chemistry and biochemistry* (pp. 145–239). Springer.
- Fu, W.-C., Opazo, M. A., Acuña, S. M., & Toledo, P. G. (2017). New route for self-assembly of α -lactalbumin nanotubes and their use as templates to grow silver nanotubes. *PLoS One*, 12(4), e0175680. <https://doi.org/10.1371/journal.pone.0175680>
- Fuciños, C., Estévez, N., Pastrana, L., Tovar, C. A., & Rúa, M. L. (2021). Biofunctionality assessment of α -lactalbumin nanotubes. *Food Hydrocolloids*, 117, 106665. <https://doi.org/10.1016/j.foodhyd.2021.106665>
- Gallochio, F., Belluco, S., & Ricci, A. (2015). Nanotechnology and food: Brief overview of the current scenario. *Procedia Food Science*, 5, 85–88.
- Giroux, H. J., Houde, J., & Britten, M. (2010). Preparation of nanoparticles from denatured whey protein by pH-cycling treatment. *Food Hydrocolloids*, 24(4), 341–346. <https://doi.org/10.1016/j.foodhyd.2009.10.013>
- Graveland-Bikker, J. F., Koning, R. I., Koerten, H. K., Geels, R. B. J., Heeren, R. M. A., & de Kruijff, C. G. (2009). Structural characterization of α -lactalbumin nanotubes. *Soft Matter*, 5(10), 2020–2026. <https://doi.org/10.1039/B815775H>
- Hernández, H. L. H., Santos, I. J. B., Oliveira, E. B. d., Teófilo, R. F., Soares, N. D. F. F., & Coimbra, J. S. D. R. (2020). Nanostructured conjugates from tara gum and α -lactalbumin. Part 1. Structural characterization. *International Journal of Biological Macromolecules*, 153, 995–1004. <https://doi.org/10.1016/j.ijbiomac.2019.10.229>
- Hu, Y., Bao, C., Li, D., You, L., Du, Y., Liu, B., Li, X., Ren, F., & Li, Y. (2019). The construction of enzymolyzed α -lactalbumin based micellar nanoassemblies for encapsulating various kinds of hydrophobic bioactive compounds. *Food & Function*, 10(12), 8263–8272. <https://doi.org/10.1039/C9FO02035G>
- Ipsen, R., & Otte, J. (2007). Self-assembly of partially hydrolysed α -lactalbumin. *Biotechnology Advances*, 25(6), 602–605. <https://doi.org/10.1016/j.biotechadv.2007.07.006>
- Kamau, S. M., Cheison, S. C., Chen, W., Liu, X.-M., & Lu, R.-R. (2010). Alpha-lactalbumin: Its production technologies and bioactive peptides. *Comprehensive Reviews in Food Science and Food Safety*, 9(2), 197–212. <https://doi.org/10.1111/j.1541-4337.2009.00100.x>
- Katouzian, I., & Jafari, S. M. (2019). 4 – Nanotubes of α -lactalbumin for encapsulation of food ingredients. In S. M. Jafari (Ed.), *Biopolymer nanostructures for food encapsulation purposes* (pp. 101–124). Academic Press. <https://doi.org/10.1016/B978-0-12-815663-6.00004-5>
- Katouzian, I., Jafari, S. M., Maghsoudlou, Y., Karami, L., & Eikani, M. H. (2020). Experimental and molecular docking study of the binding interactions between bovine α -lactalbumin and oleuropein. *Food Hydrocolloids*, 105, 105859. <https://doi.org/10.1016/j.foodhyd.2020.105859>
- Kher, A., Udabage, P., McKinnon, I., McNaughton, D., & Augustin, M. A. (2007). FTIR investigation of spray-dried milk protein

- concentrate powders. *Vibrational Spectroscopy*, 44(2), 375–381. <https://doi.org/10.1016/j.vibspec.2007.03.006>
- Kimpel, F., & Schmitt, J. J. (2015). Review: Milk proteins as nanocarrier systems for hydrophobic nutraceuticals. *Journal of Food Science*, 80(11), R2361–R2366. <https://doi.org/10.1111/1750-3841.13096>
- Kolakowski, P., Dumay, E., & Cheftel, J. C. (2001). Effects of high pressure and low temperature on β -lactoglobulin unfolding and aggregation. *Food Hydrocolloids*, 15(3), 215–232. [https://doi.org/10.1016/S0268-005X\(01\)00017-0](https://doi.org/10.1016/S0268-005X(01)00017-0)
- Lajnaf, R., Gharsallah, H., Jridi, M., Attia, H., & Ayadi, M. A. (2020). Antioxidant and antibacterial activities, interfacial and emulsifying properties of the apo and holo forms of purified camel and bovine α -lactalbumin. *International Journal of Biological Macromolecules*, 165, 205–213. <https://doi.org/10.1016/j.ijbiomac.2020.09.201>
- Lakowicz, J. R. (2006). Plasmonics in biology and plasmon-controlled fluorescence. *Plasmonics*, 1(1), 5–33.
- León-López, A., Pérez-Marroquín, X. A., Estrada-Fernández, A. G., Campos-Lozada, G., Morales-Peñalosa, A., Campos-Montiel, R. G., & Aguirre-Álvarez, G. (2022). Milk whey hydrolysates as high value-added natural polymers: Functional properties and applications. *Polymers*, 14(6), 1258. <https://doi.org/10.3390/polym14061258>
- Liu, F., Ma, C., McClements, D. J., & Gao, Y. (2016). Development of polyphenol-protein-polysaccharide ternary complexes as emulsifiers for nutraceutical emulsions: Impact on formation, stability, and bioaccessibility of β -carotene emulsions. *Food Hydrocolloids*, 61, 578–588. <https://doi.org/10.1016/j.foodhyd.2016.05.031>
- Liu, Z., Jiao, Y., Wang, Y., Zhou, C., & Zhang, Z. (2008). Polysaccharides-based nanoparticles as drug delivery systems. *Advanced Drug Delivery Reviews*, 60, 1650–1662.
- Madalena, D. A., Ramos, Ó. L., Pereira, R. N., Bourbon, A. I., Pinheiro, A. C., Malcata, F. X., Teixeira, J. A., & Vicente, A. A. (2016). In vitro digestion and stability assessment of β -lactoglobulin/riboflavin nanostructures. *Food Hydrocolloids*, 58, 89–97. <https://doi.org/10.1016/j.foodhyd.2016.02.015>
- Magnuson, B. A., Jonaitis, T. S., & Card, J. W. (2011). A brief review of the occurrence, use, and safety of food-related nanomaterials. *Journal of Food Science*, 76(6), R126–R133. <https://doi.org/10.1111/j.1750-3841.2011.02170.x>
- Monteiro, A. A., Monteiro, M. R., Pereira, R. N., Diniz, R., Costa, A. R., Malcata, F. X., Teixeira, J. A., Teixeira, Á. V., Oliveira, E. B., Coimbra, J. S., Vicente, A. A., & Ramos, Ó. L. (2016). Design of bio-based supramolecular structures through self-assembly of α -lactalbumin and lysozyme. *Food Hydrocolloids*, 58, 60–74. <https://doi.org/10.1016/j.foodhyd.2016.02.009>
- Nigen, M., Croguennec, T., & Bouhallab, S. (2009). Formation and stability of α -lactalbumin-lysozyme spherical particles: Involvement of electrostatic forces. *Food Hydrocolloids*, 23(2), 510–518. <https://doi.org/10.1016/j.foodhyd.2008.02.005>
- Pereira, R. N., Teixeira, J. A., Vicente, A. A., Cappato, L. P., da Silva Ferreira, M. V., da Silva Rocha, R., & da Cruz, A. G. (2018). Ohmic heating for the dairy industry: A potential technology to develop probiotic dairy foods in association with modifications of whey protein structure. *Current Opinion in Food Science*, 22, 95–101. <https://doi.org/10.1016/j.cofs.2018.01.014>
- Relkin, P., & Mulvihill, D. M. (1996). Thermal unfolding of β -lactoglobulin, α -lactalbumin, and bovine serum albumin. A thermodynamic approach. *Critical Reviews in Food Science and Nutrition*, 36(6), 565–601. <https://doi.org/10.1080/10408399609527740>
- Rodiles-López, J. O., Jaramillo-Flores, M. E., Gutiérrez-López, G. F., Hernández-Arana, A., Fosado-Quiroz, R. E., Barbosa-Cánovas, G. V., & Hernández-Sánchez, H. (2008). Effect of high hydrostatic pressure on bovine α -lactalbumin functional properties. *Journal of Food Engineering*, 87(3), 363–370. <https://doi.org/10.1016/j.jfoodeng.2007.12.014>
- Santos, I. J. B., Saraiva, C. S., Monteiro, A. A., & dos Reis Coimbra, J. S. (2019). Application and potential of nanotechnology in milk and derivatives processing industry. In *Food applications of nanotechnology* (pp. 225–249). CRC Press.
- Shi, R., Li, T., Li, M., Munkh-Amgalan, G., Qayum, A., Bilawal, A., & Jiang, Z. (2021). Consequences of dynamic high-pressure homogenization pretreatment on the physicochemical and functional characteristics of citric acid-treated whey protein isolate. *LWT*, 136, 110303. <https://doi.org/10.1016/j.lwt.2020.110303>
- Shimomura, M., & Sawadaishi, T. (2001). Bottom-up strategy of materials fabrication: A new trend in nanotechnology of soft materials. *Current Opinion in Colloid & Interface Science*, 6(1), 11–16. [https://doi.org/10.1016/S1359-0294\(00\)00081-9](https://doi.org/10.1016/S1359-0294(00)00081-9)
- Shukla, K. (2012). Nanotechnology and emerging trends in dairy foods: The inside story to food additives and ingredients. *International Journal of Nanoscience and Nanotechnology*, 1(1), 41–58.
- Souza, T. G. F., Ciminelli, V. S. T., & Mohalle, N. D. S. (2016). A comparison of TEM and DLS methods to characterize size distribution of ceramic nanoparticles. *Journal of Physics: Conference Series*, 733(1), 12039.
- Sreerama, N., & Woody, R. W. (2000). Estimation of protein secondary structure from circular dichroism spectra: Comparison of CONTIN, SELCON, and CDSSTR methods with an expanded reference set. *Analytical Biochemistry*, 287(2), 252–260. <https://doi.org/10.1006/abio.2000.4880>
- Tarhan, Ö., Hamaker, B. R., & Campanella, O. H. (2021). Structure and binding ability of self-assembled α -lactalbumin protein nanotubular gels. *Biotechnology Progress*, 37(3), e3127. <https://doi.org/10.1002/btpr.3127>
- Tarhan, Ö., & Harsa, Ş. (2014). Nanotubular structures developed from whey-based α -lactalbumin fractions for food applications. *Biotechnology Progress*, 30(6), 1301–1310. <https://doi.org/10.1002/btpr.1956>
- Walzem, R. L., Dillard, C. J., & German, J. B. (2002). Whey components: Millennia of evolution create functionalities for mammalian nutrition: What we know and what we may be overlooking. *Critical Reviews in Food Science and Nutrition*, 42(4), 353–375. <https://doi.org/10.1080/10408690290825574>
- Yang, H., Yang, S., Kong, J., Dong, A., & Yu, S. (2015). Obtaining information about protein secondary structures in aqueous solution using Fourier transform IR spectroscopy. *Nature Protocols*, 10(3), 382–396. <https://doi.org/10.1038/nprot.2015.024>
- Yu, J., Wang, Y., Li, D., & Wang, L. (2022). Freeze-thaw stability and rheological properties of soy protein isolate emulsion gels induced by NaCl. *Food Hydrocolloids*, 123, 107113. <https://doi.org/10.1016/j.foodhyd.2021.107113>

- Zhang, H., Yu, D., Sun, J., Guo, H., Ding, Q., Liu, R., & Ren, F. (2014). Interaction of milk whey protein with common phenolic acids. *Journal of Molecular Structure*, 1058, 228–233. <https://doi.org/10.1016/j.molstruc.2013.11.009>
- Zhong, H., Gilmanshin, R., & Callender, R. (1999). An FTIR study of the complex melting behavior of α -lactalbumin. *The Journal of Physical Chemistry B*, 103(19), 3947–3953. <https://doi.org/10.1021/jp984518p>

SUPPORTING INFORMATION

Additional supporting information can be found online in the Supporting Information section at the end of this article.

How to cite this article: Bianchi, J. R. D. O., Paz, B. E. R., Fonseca, L. G., Carvalho, R. L., Magalhães, J. C., Pacheco, K. A., Schlogl, A. E., Fabrino, D. L., Nucci, E. R., Sélia, J., Coimbra, J. S. D. R., & Santos, I. J. B. (2023). Cytotoxicity, structural, conformational, and techno-functional properties of α -lactalbumin nanostructured aggregates. *Journal of Food Science*, 88, 3049–3062. <https://doi.org/10.1111/1750-3841.16622>